

The eco-evolutionary impacts of collective straying on metapopulation dynamics

Justin D. Yeakel^{1,2,*}, Jean Philippe Gibert¹, Peter A. H. Westley³, & Jonathan W. Moore⁴

¹School of Natural Sciences, University of California, Merced, Merced CA, USA

²The Santa Fe Institute, Santa Fe NM, USA

³College of Fisheries and Ocean Sciences, University of Alaska, Fairbanks, Fairbanks AK, USA

⁴Earth2Oceans Research Group, Simon Fraser University, Vancouver BC, Canada

*To whom correspondence should be addressed: jdyeakel@gmail.com

I. INTRODUCTION

Intraspecific diversity can increase the resilience and stability of species or metapopulations. This diversity-stability linkage can occur when there are asynchronous population dynamics, where the changes in population size vary across a metapopulation. This asynchrony will increase the potential for demographic rescue [1] and also decrease the variability of processes that integrate across the metapopulation [2]. For example, different responses to climate variability within populations of a rare plant reduced abundance fluctuations [3]. This statistical buffer has traditionally been quantified as the Portfolio Effect (PE), which is the ratio of the population CV to the CV of the aggregated metapopulation [4].

Movement of individuals across populations (i.e., straying or dispersal) can have a large influence on metapopulation dynamics [5]. First, some level of straying is necessary to enable the rescue effect, whereby dispersal among populations can rescue small populations from local extinction (REFS). Second, high levels of straying may synchronize populations and actually increase the risk of extinction of the entire metapopulation [1]. Third, straying will influence the evolutionary dynamics of the metapopulation, however evolutionary impacts are less well understood. Although the straying of individuals into sites hosting other populations provides connections within the larger metapopulation, potentially promoting ecological and evolutionary rescue, it may also introduce maladapted individuals into habitats that are host to different environmental conditions, possibly lowering the mean fitness of the local (mixed) population [6]. Further, this straying may lead to genetic homogenization that erodes the asynchrony that underpins portfolio effects and metapopulation persistence. Thus, the dual nature of straying as both promoter of connections among metapopulation demes and potential eroder of locally adapted gene complexes highlights the interplay between ecological dynamics of connected populations and the evolutionary dynamics of mixed trait distributions that respond to heterogeneous local conditions.

Migratory populations that return to a breeding ground or natal stream to reproduce are linked to each other by some proportion of the population that permanently disperse, or stray into the ‘wrong’ site; we might say that there is at least one *Kevin* in every school or flock (figure 1). There is growing appreciation that the

rate of straying may be influenced by abiotic, biotic, and anthropogenic factors [7–9]. Recently the role of social interactions and collective navigation has been hypothesized [This issue]. The rate at which individuals stray, m , may be linked to errors made at an individual-level that are themselves diminished by migrating in groups and pooling individual choices [10, 11]. Regardless of the mechanism’s governing straying, the effect that it has on the dynamics of individual populations and the metapopulation as a whole is a topic of considerable interest that has tangible conservation implications [12–14]. Whether, and to what extent, the ecological consequences of straying depend on the evolutionary dynamics that emerge from populations distributed across a selective gradient is unclear. How the assumed negative evolutionary effects of straying and subsequent gene flow is balanced by the positive effects of demographic rescue is the subject of this contribution.

That evolutionary forces of selection and gene flow play out heterogeneously across geographic mosaics is now a foundational concept in ecology and evolutionary biology [15–18]. These mosaics are in part driven by environmental differences between habitats that alter the selective forces acting on different phenotypes [19], and a principle underlying assumption is that there is gene flow such that individuals from different habitats mix over space [20–26]. Although the evolutionary outcomes of these spatial processes have been explored in depth (REFS), it is less well understood how selective mosaics and their consequent evolutionary forces impact population dynamics as they unfold [27]. How the ecological dynamics of phenotypically diverse metapopulations, wherein constituent populations are subject to different selective regimes, are altered affected by evolutionary forces is less well known.

The eco-evolutionary impacts of straying likely has important implications for conservation and management in key taxa such as in salmon. Salmon may operate as metapopulations, where populations are genetically distinct but linked by some level of straying [28, 29]. Asynchrony among salmon populations also increases the stability of fisheries that integrate across this diversity [30, 31]. However, these portfolio effects may be eroded if asynchrony is influenced by genetic diversity and this genetic diversity is lost. Braun et al. [32] found that genetic differences among populations of Chinook salmon was correlated with the degree of asynchrony in population dynamics. Artificial propagation of salmon by

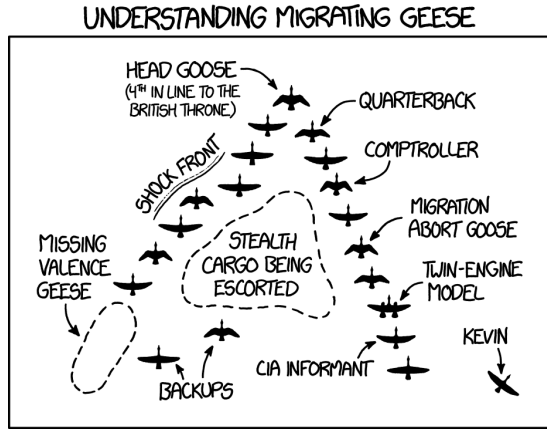


Figure 1: *Migrating Geese*, a comic from Randall Monroe’s xkcd (<https://xkcd.com/1729/>). A flock of geese travel in the direction of a shared destination, the lone stray named *Kevin*. In this case, the rate of straying is $m = 0.05$, which is not an uncommon rate for migrating populations of salmon [45]. Reprinted under the Creative Commons Attribution-NonCommercial 2.5 License.

hatcheries and their strays may erode local genetic diversity, asynchrony among populations, and portfolio effects [33–35]. While anadromous salmonid fishes (genera *Oncorhynchus* and *Salmo*) are reknown for returning to their natal spawning habitats with high accuracy and precision after years at sea [8, 36, 37], there are generally some individuals that ‘stray’ to non-natal sites to spawn [38, 39]. Although extensive work has been done to document the extent of straying from donor populations and into recipient populations [8, 9], only recently have the abiotic, biotic, and anthropogenic influences of ‘straying’ behaviors been investigated systemically [40–42]. Most recently the role of social interactions and collective navigation has been hypothesized [10, 11]. These strays can introduce new maladaptive genotypes into the recipient population. Straying among salmon may be influenced by environmental factors such as water temperature, human activities such as hatchery practices, and population density as predicted by the collective migration hypothesis [43]. Thus, there is an opportunity to consider the eco-evolutionary consequences of straying for metapopulations in species of conservation and management concern such as salmon [44].

Here we seek to explore how the potentially detrimental evolutionary effects of straying (erosion of local adaptation) and subsequent gene flow is balanced by the positive effects of demographic rescue is the subject of this contribution. To address this question we construct a minimal eco-evolutionary model of two populations occupying different sites that are linked by straying individuals, each of which with an associated trait distribution subject to natural selection determined by local conditions. [We show that taking straying into account leads to alternative stable states in population densities and trait values, which has consequences for maladaptation,

intraspecific trait variability, and long-term sustainability of salmon metapopulations.]

II. MODEL DESCRIPTION & ANALYSIS

(a) Metapopulation framework

We consider two populations N_1 and N_2 that inhabit two distinct habitats, each with trait values x_1 and x_2 determining recruitment rates. We assume that there is an optimum trait value θ_1 and θ_2 associated with each habitat, where recruitment is maximized if the trait value of the local population equals the optimum, such that $x = \theta$. Moreover, we assume that $x_{1,2}$ are normally distributed with means μ_1 and μ_2 and have the same standard deviation σ . As such, the recruitment rate for both populations is determined by the mean trait value of the local population, such that $r_1 = R_1[\mu_1(t), \theta_1]$. Trait means for each population are subject to selection, the strength of which depends on the difference between the trait mean and the local trait optimum at a given point in time [46, 47].

The two populations are assumed to reproduce in spatially separate sites that are close enough such that a proportion of the population m can stray into the other site, and where mortality occurs before individuals return to reproduce. If there is no straying between these populations (such that they are independent), then the mean trait evolves towards the optimal value such that $x_1 \rightarrow \theta_1$, and the recruitment rate for that population will be maximized. If there is straying between populations at rate m , then the traits in each respective location will be pulled away from the optimum, and recruitment rates will be lowered. As $m \rightarrow 0.5$, the populations are perfectly mixed, acting as a single population.

We use the discrete Ricker population dynamic framework described by Shelton and Mangel [48] as the basis for our two-site model, with the added effect of the local population N_i mixing with a set proportion m of a remote population N_j that is straying into it. In this sense, both populations serve as donor and recipient populations. We first assume that the proportion e^{-Z} of both populations survive such that the surviving aggregated population, composed of both local individuals (at site i) and incoming strays (from site j), is $((1 - m)N_i(t) + mN_j(t))e^{-Z}$. Because local individuals will recruit differently than incoming strays, the recruitment of the aggregate must incorporate two recruitment functions, given by $(R_i[\mu_i(t)](1 - m)N_i(t) + R_i[\mu_j(t)]mN_j(t))$. This mix of individuals is subject to the same compensatory effects, which is determined by the parameter β . Taken together, the difference equation that determine changes in population size is

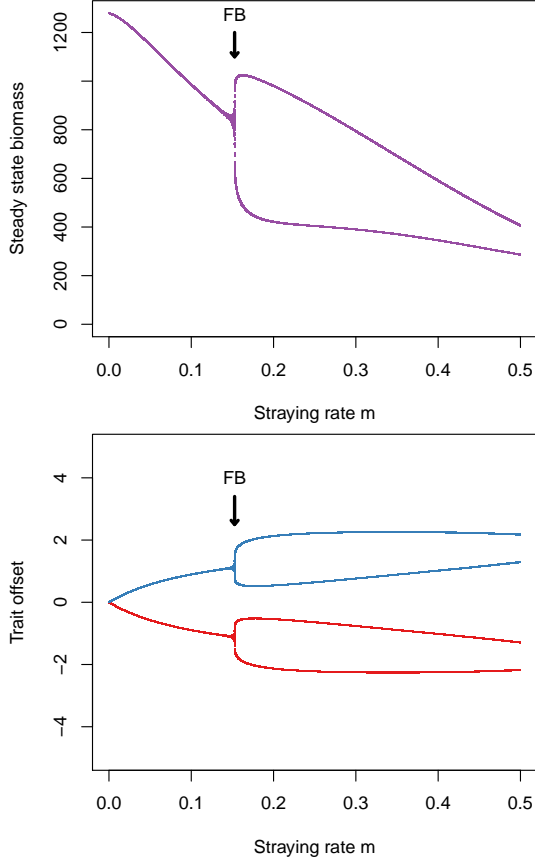


Figure 2: A) The steady state densities of N_1 and N_2 as a function of a constant stray rate m . Which population attains the low- or high-density state is random due to small applied fluctuations in the initial conditions. B) The steady state trait values measured as $\theta_i - x_i$, as a function of a constant stray rate m .

$$\begin{aligned}
 N_i(t+1) = & \\
 & ((1-m)N_i(t) + mN_j(t))e^{-Z} \\
 & + (R_i[\mu_i(t)](1-m)N_i(t) + R_i[\mu_j(t)]mN_j(t)) \\
 & \times e^{-\beta((1-m)N_i(t) + mN_j(t))},
 \end{aligned} \tag{1}$$

where the difference equation for N_j mirrors that for N_i .

The recruitment of local individuals $(1-m)N_i(t)$ as a function of their mean trait value at time t and the local trait optimum, is

$$\begin{aligned}
 R_i[\mu_i(t)] = & \\
 & \int_{-\infty}^{\infty} r_{\max} \exp \left\{ -\frac{(x_i(t) - \theta_i)^2}{2\tau^2} \right\} \text{pr}(x_i(t), \mu_i, \sigma^2) dx_i(t) + \tilde{P} \\
 & = \frac{r_{\max}\tau}{\sqrt{\sigma^2 + \tau^2}} \exp \left\{ -\frac{(\theta_i - \mu_i(t))^2}{2(\sigma^2 + \tau^2)} \right\} + \tilde{P},
 \end{aligned} \tag{2}$$

where the mismatch between the local trait mean $\mu_i(t)$ and the local optimum θ_i scales the recruitment rate for

the population, and $\tilde{P} \sim \text{Normal}(0, 0.01)$ introduces a small amount of demographic error. The parameter τ is the strength of selection, and controls the sensitivity of recruitment to changes in the mean trait value away from the optimum (the strength of selection increases with smaller values of τ), which we set as $\tau = 1$ here and throughout. Because straying individuals are emigrating from a population with a mean trait value farther from the local optimum, their rate of recruitment is diminished, and this matches what is observed in wild populations [43].

Because individuals from the local population are mixed with individuals from the remote population via straying and subsequent reproduction, the resulting trait distribution is a mixed normal with weights corresponding to the proportion of the mixed population that are local individuals, w_i , and for the straying individuals, $1 - w_i$, where

$$w_i = \frac{(1-m)N_i(t)}{(1-m)N_i(t) + mN_j(t)}. \tag{3}$$

We make two simplifying assumptions. First, we assume that the distribution resulting from the mix of remote and local individuals, following reproduction, is also normal with a mean value equal to that of the mean for the mixed-normal distribution. Second, we assume that changes in trait variance through time are minimal, such that σ^2 is assumed to be constant, and this is a common simplification in eco-evolutionary models of population dynamics [47, 49, 50].

An increasing flow of incoming strays is generally expected to pull the mean trait value of the local population away from its optimum over time, which will decrease its rate of recruitment. Following Lande [47], the mean trait value thus changes through time according to the difference equation

$$\begin{aligned}
 \mu_i(t+1) = & w_i\mu_i(t) + (1-w_i)\mu_j(t) \\
 & + h^2\sigma^2 \frac{\partial}{\partial \mu_i} \ln(w_i R_i[\mu_i(t)|\theta_i] + (1-w_i)R_i[\mu_j(t)|\theta_i]),
 \end{aligned} \tag{4}$$

where the first two factors determine the mixed normal average of the aggregated local and remote populations. The partial derivative in the Eq. 4 determines how the mean trait changes through time due to natural selection [47], which is proportional to the change in mean fitness with respect to μ_i .

(b) Measuring metapopulation robustness We evaluated metapopulation robustness by measuring the average-CV portfolio effect (PE) [29, 51] as well as the time required for the system to return to a steady state following an induced disturbance to one or both of the populations [52]. The average-CV portfolio effect is, as the name implies, the average CV across each population divided by the CV of the aggregate [53], such that

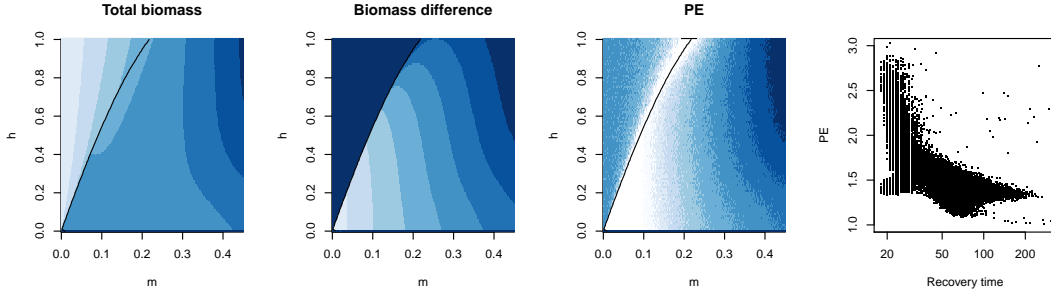


Figure 3: (a) Total means N_t , (b) difference in means ΔN , and (c) the portfolio effect PE as a function of heritability h^2 and a constant stray rate m . Light colors = high values. The black line shows the fold bifurcation separating a single steady state (left) from alternative steady states (right). (d) The relationship between the time to recovery following a disturbance and the portfolio effect.

$$\langle \text{PE} \rangle = \frac{1}{X} \sum_{i=1}^X \frac{\sqrt{\text{VAR}(N_i)}}{E(N_i)} \cdot \frac{E(N_T)}{\sqrt{\text{VAR}(N_T)}}, \quad (5)$$

where in this case the number of populations is limited to $X = 2$ and the expectations $E(\cdot)$ and variances $\text{VAR}(\cdot)$ are evaluated at the steady state. As the CV of N_T decreases relative to that of the constituent populations, $\langle \text{PE} \rangle > 1$, and the metapopulation is presumed to become more stable. Portfolio effects greater than unity corresponds to less synchronization [29, 54, 55] and thus a greater potential for demographic rescue among populations, buffering the system as a whole against extinction.

A more direct way to measure system robustness is to measure the time that it takes the system (measured as the aggregate biomass N_T) to recover its steady state abundance following an induced disturbance: systems that recover quickly (shorter recovery times) are more robust than those that recover more slowly (longer recovery times). Although there is a direct eigenvalue relationship between the rate of return following a small pulse perturbation [56], because we aimed to 1) assess the effects of a large perturbation, and 2) estimate the time required for all transient effects to decay (including dampened oscillations), we used a simulation-based numerical procedure.

Numerically estimating the time that it takes for a perturbed system to relax also permits a more detailed perspective of metapopulation fragility. For example, if populations settle to alternative steady states (alternative steady states in our model requiring one population to be high-density and one low-density), comparing recovery times after a disturbance applied to the high, low, and/or both populations allows for an assessment of which component of the metapopulation has a longer-lasting influence on the system's recovery. We measured the time required for the system N_T to recover to its steady state following three types of induced disturbance: (i) extinction of the low-density population; (ii) extinction of the high-density population (scenarios i and ii

are equivalent if the system is in the single steady state regime); (iii) near-collapse of both populations where just 1.0% of each survives. Throughout, we will refer to an increase in the portfolio effects and/or reduction in recovery times as promoting metapopulation robustness, which is expected to have a positive effect on persistence.

(c) The effects of density and distance on the rate of straying We have so far assumed that the proportion of strays leaving and entering a population is constant, however there is mounting evidence that at least in some species (including straying) the straying rate is density dependent with a signature of collective navigation [9, 11]. Specifically, the rate at which individuals stray has been linked directly to a collective decision-making phenomenon, where greater numbers of individuals tend to decrease the rate at which individuals err, reducing the overall proportion of a population that strays. According to Berdahl et al. [11, 57], given the probability that an individual strays is m_0 , the proportion of the local population $N_i(t)$ that strays is

$$m(t) = m_0 \left(1 - \frac{N_i(t)}{C + N_i(t)} \right), \quad (6)$$

where C is a half-saturation constant. We note that at the limit $C \rightarrow \infty$, the density dependent straying rate becomes constant such that $m(t) \rightarrow m_0$, and this corresponds to the original formulation where $m = m_0$. A similar observation shows that when the population density is very high, $m(t) \rightarrow 0$, and when it is small, individuals operate without regard to collective behavior, meaning $m(t) \rightarrow m_0$. Thus, for realistic population densities, $m(t) < m_0$.

The straying rate is largely influenced by the distance between the donor and recipient population. The greater the distance between two populations, the lower the expected rate of straying [7, 41]. We account for this interdependence in our model by assuming that m (if the stray rate is constant) or m_0 (if the stray rate is density dependent) is a function of the difference between

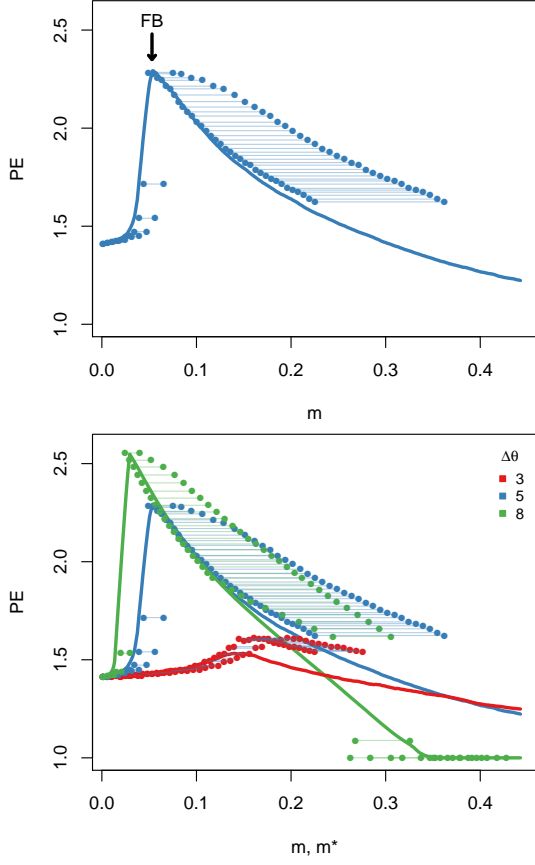


Figure 4: (a) Median portfolio effect as a function of a constant stray rate m (solid line) and density dependent stray rate (point pairs) given heritability is $h^2 < 0.5$ and $\Delta\theta = 5$. Point pairs connected by a horizontal line represent the PE as a function of density dependent straying rates, evaluated for both low- and high-density populations at equilibrium. The lower straying rate of a pair is for the larger population; the higher straying rate is for the smaller population. (b) Median portfolio effects for habitats with increasing heterogeneity as measured by the difference in regional trait optima $\Delta\theta$ for both constant and density dependent stray rates as shown in (a).

optimal trait values between sites $\theta_i - \theta_j$, which can be assumed to be large if the remote site j is a great distance away from the local site i . If sites i and j are very close, the stray rate is maximized at $m_{\max} = 0.5$, assuming both sites are equally attractive to the respective populations. Thus, we can integrate these two variables by setting $m, m_0 = (1/m_{\max} + \epsilon(\theta_i - \theta_j))^{-1}$, where ϵ sets the sensitivity of a declining m to increasing distance (greater values of $\theta_i - \theta_j$).

III. RESULTS

(a) Nonlinear effects of straying on the portfolio effect and recovery time

Regardless of density dependence, straying lowers steady

state densities for both populations by (i) the donor population losing locally-adapted individuals to the recipient population and (ii) the introduction of maladapted individuals to the recipient population from the donor population (Fig. 2). This prediction is in accordance with observations from natural populations [9]. The decline in steady state densities is not gradual: as straying increases, the system crosses a fold bifurcation whereby the single steady state for the metapopulation bifurcates into two alternative steady states: one at high biomass, and one at low biomass density (figure 2a, 3a). Mean trait values for both populations bifurcate similarly (figure 2b), depending on which population attains a low- vs. high-density. Above the threshold straying rate defined by the fold bifurcation, there are two alternative eco-evolutionary states: the *dominant state* population will have a higher density and higher degree of local adaptation (lower trait offset from the local optimum), while the *subordinate state* population will have lower density with maladapted trait values (higher trait offset from the local optimum). Whether a specific population goes to one state or the other in our model is random, which is due to a small amount of introduced variance in the initial conditions.

Trait heritability has a large impact on the degree to which straying rate affects both the aggregate population steady state density ($N_T^* = N_1^* + N_2^*$; figure 3a) as well as the difference between steady state densities (the distance between alternative stable states: $\Delta N = |N_1^* - N_2^*|$; figure 3b). Greater trait heritability results in a faster decline in N_T^* with increasing straying rates m , but leads to only moderate changes to ΔN . Conversely, in the context of lower trait heritability, an increase in the straying rate has little impact on the total biomass density but contrastingly large effects on ΔN . The fold bifurcation (the black line in Figs. 3a-c) occurs at lower values of the straying rate m with decreased trait heritability h^2 (Fig 3a,b), indicating that weaker coupling between ecological and evolutionary dynamics in addition to higher rates of straying promotes the appearance of alternative stable states. Although trait heritability among salmonids is variable, most life history traits have an $h^2 < 0.5$ [33], and we largely focus additional analyses on that range.

As the fold bifurcation is approached with increasing m , the portfolio effect increases sharply due to an amplification in variance within both donor and recipient populations $\text{VAR}(N_{i,j})$. This variance increase is the product of a dynamical process known as *critical slowing down* that occurs near fold bifurcations [58], a phenomenon that some have suggested may serve as an early warning indicator for approaching phase transitions [58–61]. For larger values of m (to the right of the fold bifurcation in Fig 3a-c), where alternative steady states occur, the portfolio effect declines steadily as the CV of N_T increases. The decline over m is more gradual if trait heritability is low, and steeper if trait heritability is high (figure 3c).

If we assume that the rate of straying is density dependent, the probability that an individual strays m_0

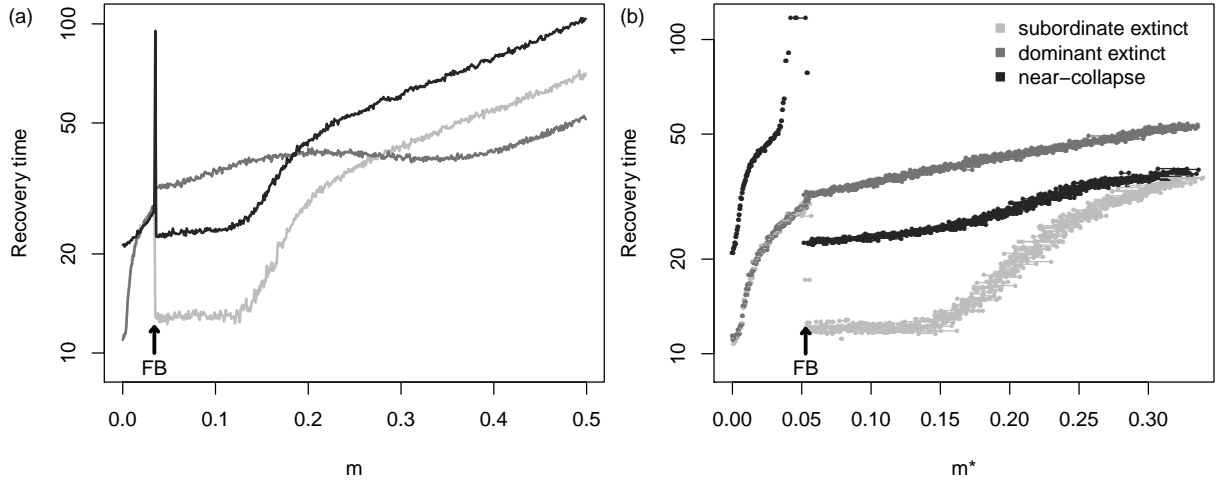


Figure 5: Recovery time of N_T following the extinction of either the low-density (light gray) or high-density (gray) population, or the near-collapse of both (dark gray) assuming (a) constant straying rates m and (b) density dependent straying rates (evaluated at the steady state m^*) with trait heritability $h^2 = 0.2$. If m is density dependent, in the alternative steady state regime there are two straying rates observed: one each for the low- and high-density populations, respectively, which are linked by a horizontal line.

determines the rate of straying within the population, such that $m(t)$ becomes lower as $N(t)$ increases, likely due to the effects of collective decision-making [11] (Eq. 6). Density dependence alters the straying rate at steady state population densities because $0 < m^* < m_0$, and this serves to rescale both the strength of the PE as well as the recovery time, but does not change the qualitative nature of our findings. In the alternative stable state regime, because each population exists at different steady state densities, there are likewise two alternative straying rates (m_i^*, m_j^*): the higher straying rate is associated with the low-density population, and the lower straying rate is associated with the high-density population. We assessed metapopulation robustness across a range of (m_i^*, m_j^*) values by varying the probability that an individual strays m_0 , which is positively and linearly related to (m_i^*, m_j^*). We find that the portfolio effects generated in systems with density dependent straying are qualitatively similar to systems with constant straying, however there are some important quantitative differences. First, the PE associated with the high-density (low m^*) population is the same as that for a system with a constant m (figure 4a). As m^* increases, we observe an increase in the PE than for systems with constant m .

As the portfolio effect is highly sensitive to the rate of straying between populations, so is the time required for the system to recover to a steady state following a large disturbance. In general, we find that the average-CV portfolio effect is negatively correlated with recovery time (figure 3d), indicating that, for our system, both measures are valuable indicators of metapopulation robustness. Because we can assess the time to recovery in response to the various disturbance types described above, this allows us to gain an in-depth perspective into the fragility of the metapopulation as a function of stray-

ing rate.

Straying had non-linear impacts on the recovery time of populations. When the dominant state (well adapted and high density) is wiped out, high levels of straying allow it to recover quickly (figure 5a) because the surviving population has a mean trait value skewed towards the optimum of the recovering population (figure S2). Yet, as straying decreases, recovery time for the disturbed dominant state population increases, in part because there is enough time for the trait distribution to move back towards the trait optimum of the subordinate state population. In contrast, when the subordinate state population (maladapted and low density) is wiped out, recovery rates are fastest at low to intermediate levels of straying. Because the mean trait values of both populations are skewed towards those of the dominant population, when the subordinate population collapses under high rates of straying, selection against the flood of maladapted individuals that stray into the recovering population extends the length of time required for it to return to its steady state (figure S1). When both populations are both dramatically reduced, recovery time is generally fastest at lower levels of straying, while near the onset of the fold bifurcation, recovery time increases explosively and this is – as the name implies – characteristic of *slowing* dynamics that occur near critical transitions [58, 62].

Density-dependent straying alters these recovery times (figure 5b). First, in comparison with constant stray rates, density-dependent straying made recovery more rapid at elevated stray rates when both populations collapsed and when the subordinate population was extirpated. At low straying rates, near-collapse of both populations resulted in longer than expected recovery times, whereas in the alternative stable state regime (higher m^*), the recovery times for different disturbance types

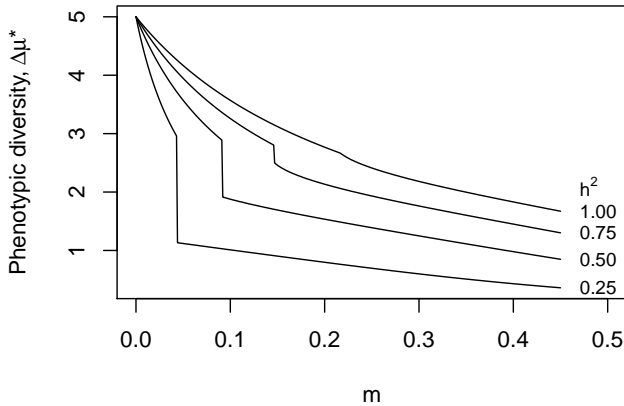


Figure 6: Phenotypic diversity ($\Delta\mu^*$) evaluated at the steady state as a function of straying rate m and trait heritability h^2 . The discrete jump occurs as the system crosses the fold bifurcation; lower phenotypic diversity emerges with higher straying rates and in the alternative steady state regime.

were very similar to systems with a constant m (figure 5b; note difference in x-axis scales). As trait heritability increased, the metapopulation always recovered more quickly if the small population was lost (figure S3). The lower recovery time for systems with increased m^* mirrors an elevated PE with higher density dependent straying rates (figure ??). In tandem, analysis of both PE and recovery time suggests that although density-dependent straying does not appear to change the ‘dynamic landscape’ in our minimal model, it does appear to promote robustness, particularly when the aggregate biomass is low and straying is correspondingly high.

Increased rates of straying lowers phenotypic diversity ($\Delta\mu^* = |\mu_i(t) - \mu_j(t)|$, evaluated at the steady state) because both local and remote populations are increasingly homogenized. The loss of phenotypic diversity with increased straying is greater if trait heritability is low because traits take longer to go back to their local optima than they do when heritability is large. Hence straying counters the effect of diversifying local adaptation. Less intuitively, we observe a discrete jump towards low phenotypic diversity as the fold bifurcation is crossed (figure 6). Although the development of alternative stable states elevates the portfolio effect due to the variance-dampening effects of the aggregate, entering this dynamic regime also results in a substantial decline in phenotypic diversity, which may have less predictable adverse effects on the population.

(b) The influence of habitat heterogeneity on metapopulation robustness

Increasing differences in optimal trait values between

sites ($\Delta\theta = |\theta_i - \theta_j|$) corresponds to greater regional differences in the conditions that favor alternative trait complexes, which we interpret here as greater habitat heterogeneity (REFS). If both populations are isolated, natural selection will direct the mean trait values of both populations towards their respective optima, such that $\mu_i(t) \rightarrow \theta_i$ as $t \rightarrow \infty$. With the onset of straying, we find that increasingly divergent trait optima generally lower N_T and exaggerate ΔN (figure S4), such that the biomass distribution becomes increasingly uneven. The impact of habitat heterogeneity on the portfolio effect and recovery time is more complex, serving to emphasize the nonlinear relationship between rates of straying and metapopulation robustness. As habitat heterogeneity increases, alternative stable states appear at lower straying rates – with the crossing of the fold bifurcation, accompanied by a peak in the PE – whereas the magnitude of increase in the PE also increases (figure 4b), reducing recovery time (figure S5). For increased rates of straying, greater habitat heterogeneity erodes the PE (figure 4b) and increases the recovery time (figure S5). These results together suggest that habitat heterogeneity, as measured as the differences in trait optima between two habitats $\Delta\theta$, promotes robustness when straying rates are low, and erodes robustness when straying rates are high.

(c) Distance dependent straying and habitat heterogeneity

We have so far treated $\Delta\theta$ and m as independent parameters, however we may also assume that if environmental heterogeneity increases with distance, the rate of straying may be expected to decline with habitat heterogeneity, given that individuals will stray less into distant habitats. Alternatively, individuals may be less likely to stray into very different habitats due to the influence of environmental cues on individual decision-making (REFS?). If we incorporate this interdependence of m and $\Delta\theta$, low rates of straying correspond to mixing dissimilar (distant) populations, and high rates of straying would correspond to mixing similar (nearby) populations.

We find that alternative stable states now appear for very low rates of straying $0 < m \leq 0.43$, corresponding to greater habitat heterogeneity $\Delta\theta$. As the straying rate increases, a single stable state emerges as the fold bifurcation is crossed. As straying increases (now the single steady state regime), the time required for recovery following extinction of either the population declines (to the right of figure 7). However, as straying decreases the system crosses the fold bifurcation, entering the alternative steady state regime (to the left in figure 7). At low rates of straying, there is a small amount of mixing between dissimilar (distant) populations. Here we find that if the subordinate population is wiped out, the time to recovery is minimized, whereas if the dominant population is wiped out, the time to recovery is maximized; near-collapse of both results in intermediate recovery times.

When straying rates are low and the difference in trait

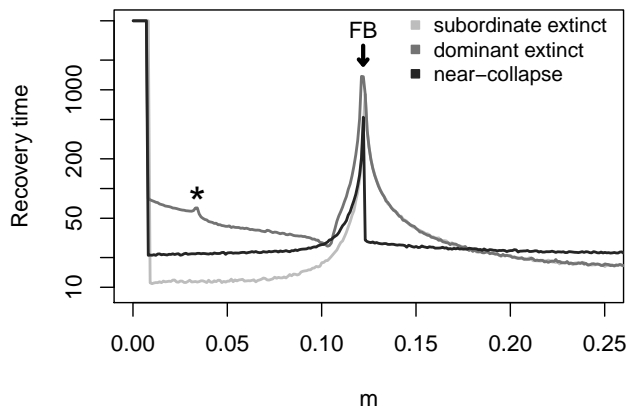


Figure 7: Distance dependent recovery times for three disturbance types. When straying is distance dependent, m increases as $\Delta\theta$ decreases.

optima are correspondingly high, we might presume that extinction of the dominant population would result in relatively faster recovery. This would be a logical assumption because the mean trait value of the subordinate population is skewed towards that of the dominant (larger) population, such that recruitment at the disturbed site would be high. Our results show, however, that this assumption is wrong: although the mean trait value of the subordinate population *is* skewed towards the optimum of the dominant population, when the latter is wiped out and the rate of straying is low, there is enough time and isolation for the subordinate trait mean to shift towards its own optimum, and away from that of the recovering dominant population (figure S7). This *selective inertia* occurs until the dominant population grows large enough that the evolving subordinate phenotype is overwhelmed by incoming strays, shifting it back towards that of the now-recovered dominant population. Importantly, this effect can lead to much longer recovery times for the dominant population, as well as a switch in which population is dominant/subordinate (a switch in who occupies the alternative states), when the straying rate is very low (and $\Delta\theta$ is large). The threshold value of m , below which this behavior occurs, is marked by the asterisk in figure 7. These results hold for both constant and density dependent straying rates (figure S8)

IV. DISCUSSION

We have shown that dispersal between populations, coupled with localized selection against donor phenotypes, has a large and nonlinear impact on dynamic properties that directly impacts metapopulation robustness, and by extension persistence. Although there are various

ways to measure ‘robustness’ (REF:TREE), we employ two measures: 1) the average-CV portfolio effect, a statistical metric commonly used to assess the fragility of populations; 2) the recovery time, defined here as the time required for the aggregate metapopulation biomass N_T to return to its steady state after different types of induced disturbances, which is mechanistically linked to the likelihood of persistence (REF). In our minimal model of dispersal and natural selection between two populations, we show that these phenomenological and mechanistic descriptors of metapopulation robustness are tightly coupled (figure 3d).

The immigration of dispersing individuals with trait values far from the local optimum generally lowers the combined steady state biomass N_T and increases the likelihood that the system gives way to alternative steady states, pushing one of the populations close to extinction. The formation of alternative stable states in our system is a relatively common example of spatial pattern formation, and occurs above a threshold straying rate. Pattern formation can occur as a consequence of myriad ecological processes, including habitat selection (REFS), aggregation of individuals (REFS), local environmental conditions (REFS), or interspecific interactions like competition (REFS). It is also well known to occur with the onset of spatially or diffusion-induced instabilities (Turing instabilities, REFS). Here, we describe an interesting alternative mechanism through which pattern formation in local densities can occur, when the onset of movement mediated maladaptation leads to local differences in reproductive rates that yield differences in densities that would, in the absence of straying, be the same.

To what extent the existence of alternative stable states promotes or diminishes the system as a whole is a matter of perspective. On the one hand, one population is pushed to a low-density state (figure 2) with a lower total biomass of the aggregate (figure |reffig:PEa), suggesting that the system is more fragile. On the other hand, the presence of *just enough* straying to cause formation of alternative stable states both increases the portfolio effect (figure 3c) and reduces the rate of return – particularly if straying is density dependent (figure 5c,d) as might be common in systems with collective navigation (REF). Importantly, the asymmetry in population densities also leads an asymmetry in the mean trait values between sites: because the high-density population contains the majority of biomass, the proportion of the low-density population that is composed of incoming strays is generally large, and this leads to mean trait values in both sites skewed towards that of the high-density site. This has important ramifications for metapopulation robustness, as measured by both the portfolio effect as well as recovery time.

Although the portfolio effect is negatively correlated with recovery time, there is one exception: the point of transition from a single steady state to alternative steady states, which occurs at the fold bifurcation (REF). At this point, the portfolio effect is maximized, but so is

the recovery time (figures 3, 5). This suggests that while the sharply increasing variance of the individual populations is dampened by aggregation, a large disturbance will have a much greater adverse effect due to exponentially longer recovery times. Whether the change in variance, also known as critical slowing down, as the alternative steady state regime is approached could be used as an early warning signal of an oncoming phase transition is a hotly debated topic (REFS). The detectability of such changes in dynamical behavior among salmonids appears to be idiosyncratic across species, though the difficulty in measuring critical slowing down may - ironically - be masked by large portfolio effects [63].

Previous theoretical work has shown that the largest perturbations lead to the longest recovery times [52]. In terms of relative biomass lost, the largest perturbation that we investigate is the near-collapse of both fisheries, where only 1% of the pre-perturbation population densities survive, however whether this disturbance results in the longest recovery time depends largely on the rate of straying and trait heritability. For example, when straying and trait heritability are low (figure 5a,c) the extinction of the larger population maximizes return time, whereas if straying is high, near-collapse maximizes return time. The latter is always true in the alternative stable state regime is trait heritability is high (figure 5b,d).

This issue is largely focused on the notion that straying in biological systems where movement is a function of collective navigation may be density dependent. Berdahl et al. (REF) provided a mechanistic theory for density dependent straying where the proportion of the population that strays is less than the probability that a single individual (as illustrated by *Kevin*; figure 1) takes the wrong turn. Neither the transient nor asymptotic dynamics that we describe here qualitatively differ as a function of whether the rate of straying is constant or density dependent, however we observe important quantitative differences that suggest density dependent straying may play an important role in the persistence of metapopulations over evolutionary time.

First, density dependent straying reduces the time to recovery following an induced disturbance, and this is particularly true if (i) trait heritability is low, and (ii) in the case of near-collapse of both populations (figure 5c). This dynamic emerges because although both populations are near-collapse, the mean trait values of both are skewed towards those of the high-density population. As the low-density population has also collapsed, and the mean trait values of the system favor the high-density population, it grows more quickly, recovering faster (figure S9). Second, density dependent straying increases the effective portfolio effects when the steady state straying rate is higher (for both low- and high-density populations). Third, while habitat heterogeneity is interpreted here in elevating the difference in trait optima between sites, it both increases the portfolio effect and lowers recovery time at low rates of straying, but has the opposite effect at higher rates of straying. Surprisingly, we find that density dependent straying both exaggerates the negative effects when m^* is low (marginally lower portfolio effects, but substantially longer return times; figures 4b, S5a,b) and exaggerates the positive effects when m^* is high (higher portfolio effects, and shorter return times).

HAVENT EDITED FURTHER

Trait heritability determines the coupling between ecological and evolutionary dynamics, effectively setting the strength of natural selection. Among salmon species, recruitment among local populations is highly sensitive to local climatic conditions, with temperature thought to play a central role (REFS). Populations distributed across a temperature gradient are assumed to be locally adapted to different temperature regimes, such that migration between them should take into account differential environmental effects on the recruitment of mixed populations. (author?) showed heritability 0.1-0.3. Our results show that trait heritability has large effects on both metapopulation persistence as well as phenotypic diversity, particularly in the regime of low-to-moderate straying rates.

-
- [1] D. J. D. Earn, S. A. Levin, and P. Rohani, "Coherence and conservation," *Science*, vol. 290, pp. 1360–1364, Jan. 2000.
 - [2] D. E. Schindler, J. B. Armstrong, and T. E. Reed, "The portfolio concept in ecology and evolution," *Front. Ecol. Environ.*, vol. 13, pp. 257–263, June 2015.
 - [3] R. E. Abbott, D. F. Doak, and M. L. Peterson, "Portfolio effects, climate change, and the persistence of small populations: analyses on the rare plant *Saussurea weberi*," *Ecology*, vol. 98, pp. 1071–1081, Apr. 2017.
 - [4] L. M. Thibaut and S. R. Connolly, "Understanding diversity-stability relationships: towards a unified model of portfolio effects," *Ecol. Lett.*, vol. 16, pp. 140–150, Feb. 2013.
 - [5] E. J. Milner-Gulland, J. M. Fryxell, and A. R. E. Sinclair, *Animal Migration. A Synthesis*, Oxford University Press, Jan. 2011.
 - [6] C. C. Muhlfeld, R. P. Kovach, L. A. Jones, R. Al-Chokhachy, M. C. Boyer, R. F. Leary, W. H. Lowe, G. Luikart, and F. W. Allendorf, "Invasive hybridization in a threatened species is accelerated by climate change," *Nature Climate Change*, vol. 4, pp. 620–624, July 2014.
 - [7] P. A. H. Westley and T. P. Quinn, "Rates of straying by hatchery-produced Pacific salmon (*Oncorhynchus* spp.) and steelhead (*Oncorhynchus mykiss*) differ among species, life history types, and . . .," *Canadian Journal of . . .*, vol. 70, no. 5, pp. 735–746, 2013.
 - [8] M. L. Keefer and C. C. Caudill, "Homing and straying by anadromous salmonids: a review of mechanisms and rates," *Reviews in Fish Biology and Fisheries*, vol. 24, no. 1, pp. 333–368, 2014.
 - [9] N. N. Bett, S. G. Hinch, N. J. Burnett, M. R. Donaldson,

- and S. M. Naman, "Causes and Consequences of Straying into Small Populations of Pacific Salmon," *Fisheries*, vol. 42, pp. 220–230, Mar. 2017.
- [10] A. Berdahl, C. J. Torney, E. Schertzer, and S. A. Levin, "On the evolutionary interplay between dispersal and local adaptation in heterogeneous environments," *Evolution*, vol. 69, pp. 1390–1405, June 2015.
- [11] A. Berdahl, "Collective behavior as a driver of critical transitions in migratory populations," *Movement Ecology*, vol. 4, pp. 1–12, June 2016.
- [12] R. E. Brenner, S. D. Moffitt, and W. S. Grant, "Straying of hatchery salmon in Prince William Sound, Alaska," *Environmental Biology of Fishes*, vol. 94, pp. 179–195, Feb. 2012.
- [13] R. C. Johnson, P. K. Weber, J. D. Wikert, M. L. Workman, R. B. MacFarlane, M. J. Grove, and A. K. Schmitt, "Managed Metapopulations: Do Salmon Hatchery 'Sources' Lead to In-River 'Sinks' in Conservation?," *PLoS ONE*, vol. 7, pp. e28880–11, Feb. 2012.
- [14] A. H. Fullerton, S. T. Lindley, G. R. Pess, B. E. Feist, E. A. Steel, and P. Mcelhany, "Human Influence on the Spatial Structure of Threatened Pacific Salmon Metapopulations," *Conservation Biology*, vol. 25, pp. 932–944, July 2011.
- [15] S. L. Nuismer, J. N. Thompson, and R. Gomulkiewicz, "Gene flow and geographically structured coevolution," *Proc Biol Sci*, vol. 266, pp. 605–609, Mar. 1999.
- [16] J. N. Thompson, "Specific Hypotheses on the Geographic Mosaic of Coevolution," *Am. Nat.*, vol. 153, no. S5, pp. S1–S14, 1999.
- [17] S. L. Nuismer, J. N. Thompson, and R. Gomulkiewicz, "Coevolutionary clines across selection mosaics," *Evolution*, vol. 54, pp. 1102–1115, Aug. 2000.
- [18] J. N. Thompson, *The Geographic Mosaic of Coevolution*. University of Chicago Press, June 2005.
- [19] J. A. Endler, *Natural Selection in the Wild*. Princeton University Press, 1986.
- [20] R. Gomulkiewicz, J. N. Thompson, R. D. Holt, S. L. Nuismer, and M. E. Hochberg, "Hot Spots, Cold Spots, and the Geographic Mosaic Theory of Coevolution," *Am. Nat.*, vol. 156, no. 2, pp. 156–174, 2000.
- [21] J. N. Thompson and B. M. Cunningham, "Geographic structure and dynamics of coevolutionary selection," *Nature*, vol. 417, pp. 735–738, June 2002.
- [22] S. L. Nuismer, R. Gomulkiewicz, and M. T. Morgan, "Coevolution in Temporally Variable Environments," *Am. Nat.*, vol. 162, no. 2, pp. 195–204, 2003.
- [23] S. L. Nuismer and J. N. Thompson, "Coevolutionary alternation in antagonistic interactions," *Evolution*, vol. 60, pp. 2207–2217, Nov. 2006.
- [24] S. E. Forde, J. N. Thompson, R. D. Holt, and B. J. M. Bohannan, "COEVOLUTION DRIVES TEMPORAL CHANGES IN FITNESS AND DIVERSITY ACROSS ENVIRONMENTS IN A BACTERIA-BACTERIOPHAGE INTERACTION," *Evolution*, vol. 62, pp. 1830–1839, Aug. 2008.
- [25] P. R. Guimarães Jr, P. Jordano, and J. N. Thompson, "Evolution and coevolution in mutualistic networks," *Ecol. Lett.*, vol. 14, pp. 877–885, Sept. 2011.
- [26] J. P. Gibert, M. M. Pires, J. N. Thompson, and P. R. Guimarães Jr, "The spatial structure of antagonistic species affects coevolution in predictable ways," *Am. Nat.*, vol. 182, pp. 578–591, Nov. 2013.
- [27] A. P. Hendry, *Eco-evolutionary Dynamics*. Princeton University Press, Nov. 2016.
- [28] N. Schtickzelle and T. P. Quinn, "A metapopulation perspective for salmon and other anadromous fish," *Fish Fish.*, vol. 8, no. 4, pp. 297–314, 2007.
- [29] S. C. Anderson, J. W. Moore, M. M. McClure, N. K. Dulvy, and A. B. Cooper, "Portfolio conservation of metapopulations under climate change," *Ecol. Appl.*, vol. 25, no. 2, pp. 559–572, 2015.
- [30] D. E. Schindler, R. Hilborn, B. Chasco, C. P. Boatright, T. P. Quinn, L. A. Rogers, and M. S. Webster, "Population diversity and the portfolio effect in an exploited species," *Nature*, vol. 465, pp. 609–612, Mar. 2010.
- [31] H. K. Nesbitt and J. W. Moore, "Species and population diversity in Pacific salmon fisheries underpin indigenous food security," *J. Appl. Ecol.*, July 2016.
- [32] D. C. Braun, J. W. Moore, J. Candy, and R. E. Bailey, "Population diversity in salmon: linkages among response, genetic and life history diversity," *Ecography*, vol. 39, pp. 317–328, Mar. 2016.
- [33] S. M. Carlson and T. R. Seamons, "SYNTHESIS: A review of quantitative genetic components of fitness in salmonids: implications for adaptation to future change," *Evolutionary Applications*, vol. 1, pp. 222–238, Apr. 2008.
- [34] J. W. Moore, M. McClure, L. A. Rogers, and D. E. Schindler, "Synchronization and portfolio performance of threatened salmon," *Conserv. Lett.*, vol. 3, pp. 340–348, Apr. 2010.
- [35] J. R. Griffiths, D. E. Schindler, J. B. Armstrong, M. D. Scheuerell, D. C. Whited, R. A. Clark, R. Hilborn, C. A. Holt, S. T. Lindley, J. A. Stanford, and E. C. Volk, "Performance of salmon fishery portfolios across western North America," *J. Appl. Ecol.*, vol. 51, no. 6, pp. n/a–n/a, 2014.
- [36] T. P. Quinn, *The Behavior and Ecology of Pacific Salmon and Trout*. UBC Press, Nov. 2011.
- [37] B. Jonsson and N. Jonsson, *Ecology of Atlantic Salmon and Brown Trout*. Habitat as a template for life histories, Dordrecht: Springer Science & Business Media, May 2011.
- [38] T. P. Quinn, "A review of homing and straying of wild and hatchery-produced salmon," *Fisheries Research*, vol. 18, pp. 29–44, Oct. 1993.
- [39] A. P. Hendry, T. Bohlin, B. Jonsson, and O. K. Berg, "The evolution of philopatry and dispersal: homing versus straying in salmonids," in *Evolution Illuminated* (A. P. Hendry and S. C. Stearns, eds.), Oxford University Press on Demand, 2004.
- [40] M. L. Keefer, C. C. Caudill, C. A. Peery, and S. R. Lee, "Transporting juvenile salmonids around dams impairs adult migration," *Ecol. Appl.*, vol. 18, pp. 1888–1900, Dec. 2008.
- [41] P. A. H. Westley, A. H. Dittman, E. J. Ward, and T. P. Quinn, "Signals of climate, conspecific density, and watershed features in patterns of homing and dispersal by Pacific salmon," *Ecology*, vol. 96, pp. 2823–2833, Oct. 2015.
- [42] M. H. Bond, P. A. H. Westley, A. H. Dittman, D. Holecek, T. Marsh, and T. P. Quinn, "Combined effects of barge transportation, river environment, and rearing location on straying and migration of adult snake river fall-run chinook salmon," *Transactions of the American Fisheries Society*, vol. 146, pp. 60–73, Dec. 2016.
- [43] D. A. Peterson, R. Hilborn, and L. Hauser, "Local adap-

- tation limits lifetime reproductive success of dispersers in a wild salmon metapopulation,” *Nature Communications*, vol. 5, p. 3696, Apr. 2014.
- [44] S. M. Carlson, W. H. Satterthwaite, and I. A. Fleming, “Weakened portfolio effect in a collapsed salmon population complex,” *Can. J. Fish. Aquat. Sci.*, vol. 68, pp. 1579–1589, Sept. 2011.
- [45] W. H. Satterthwaite, S. M. Carlson, and I. Bradbury, “Weakening portfolio effect strength in a hatchery-supplemented Chinook salmon population complex,” *Can. J. Fish. Aquat. Sci.*, vol. 72, pp. 1860–1875, Dec. 2015.
- [46] G. G. Simpson, *The major features of evolution*. Simon and Schuster, 1953.
- [47] R. Lande, “Natural Selection and Random Genetic Drift in Phenotypic Evolution,” *Evolution*, vol. 30, p. 314, June 1976.
- [48] A. O. Shelton and M. Mangel, “Fluctuations of fish populations and the magnifying effects of fishing,” *Proc. Natl. Acad. Sci. USA*, vol. 108, pp. 7075–7080, Apr. 2011.
- [49] S. J. Schreiber, R. Bürger, and D. I. Bolnick, “The community effects of phenotypic and genetic variation within a predator population,” *Ecology*, vol. 92, pp. 1582–1593, Aug. 2011.
- [50] J. P. Gibert, A. I. Dell, J. P. DeLong, and S. Pawar, “Scaling-up trait variation from individuals to ecosystems,” *Advances in Ecological Research*, vol. 52, pp. 1–17, 2015.
- [51] D. E. Schindler, J. B. Armstrong, and T. E. Reed, “The portfolio concept in ecology and evolution,” *Front. Ecol. Environ.*, vol. 13, pp. 257–263, June 2015.
- [52] O. Ovaskainen and I. Hanski, “Transient Dynamics in Metapopulation Response to Perturbation,” *Theor. Popul. Biol.*, vol. 61, pp. 285–295, May 2002.
- [53] S. C. Anderson, A. B. Cooper, and N. K. Dulvy, “Ecological prophets: quantifying metapopulation portfolio effects,” *Methods Ecol. Evol.*, vol. 4, no. 10, pp. 971–981, 2013.
- [54] M. Loreau and C. de Mazancourt, “Species Synchrony and Its Drivers: Neutral and Nonneutral Community Dynamics in Fluctuating Environments,” *Am. Nat.*, vol. 172, pp. E48–E66, Aug. 2008.
- [55] J. D. Yeakel, J. W. Moore, P. R. Guimarães Jr, and M. A. M. de Aguiar, “Synchronisation and stability in river metapopulation networks,” *Ecol. Lett.*, vol. 17, no. 3, pp. 273–283, 2014.
- [56] J. Guckenheimer and P. Holmes, *Nonlinear Oscillations, Dynamical Systems, and Bifurcations of Vector Fields*. New York: Springer, 1983.
- [57] A. Berdahl, P. A. H. Westley, S. A. Levin, I. D. Couzin, and T. P. Quinn, “A collective navigation hypothesis for homeward migration in anadromous salmonids,” *Fish. Fish.*, vol. 17, pp. 525–542, June 2014.
- [58] M. Scheffer, J. Bascompte, W. A. Brock, V. Brovkin, S. R. Carpenter, V. Dakos, H. Held, E. H. van Nes, M. Rietkerk, and G. Sugihara, “Early-warning signals for critical transitions,” *Nature*, vol. 461, pp. 53–59, Sept. 2009.
- [59] S. J. Lade and T. Gross, “Early warning signals for critical transitions: A generalized modeling approach,” *PLoS Comp. Biol.*, vol. 8, no. 2, p. e1002360, 2012.
- [60] C. Boettiger, N. Ross, and A. Hastings, “Early warning signals: the charted and uncharted territories,” *Theor. Ecol.*, vol. 6, pp. 255–264, Aug. 2013.
- [61] V. Dakos and J. Bascompte, “Critical slowing down as early warning for the onset of collapse in mutualistic communities,” *Proc. Natl. Acad. Sci. USA*, vol. 111, pp. 201406326–17551, Nov. 2014.
- [62] C. Kuehn, “A mathematical framework for critical transitions: Bifurcations, fast-slow systems and stochastic dynamics,” *Physica D*, vol. 240, no. 12, pp. 1020–1035, 2011.
- [63] M. Krkošek and J. M. Drake, “On signals of phase transitions in salmon population dynamics,” *Proc. Roy. Soc. B*, vol. 281, pp. 20133221–20133221, Apr. 2014.

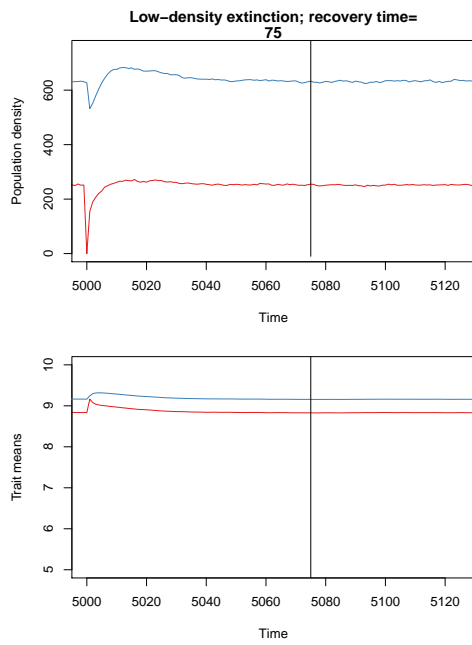


Figure S1: Extinction of low-density population with a high constant straying rate $m = 0.4$ and low trait heritability $h^2 = 0.2$ (see figure 5a). Black line marks the calculated point of recovery post-perturbation. Trait optima are $\theta_1 = 10$ (blue population trajectory) and $\theta_2 = 5$ (red population).

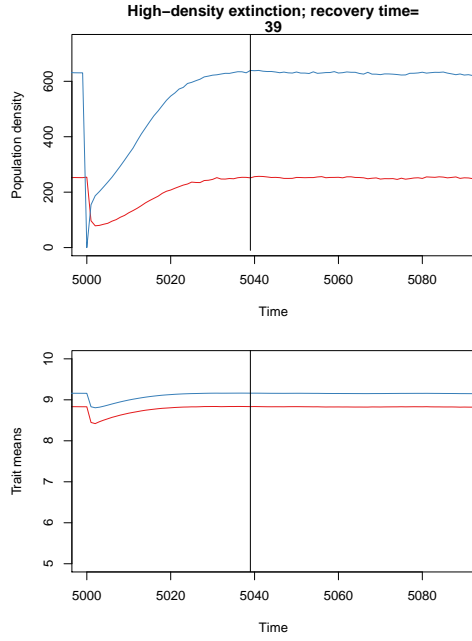


Figure S2: Extinction of high-density population with a high straying rate $m = 0.4$ and low trait heritability $h^2 = 0.2$ (see figure 5a). Black line marks the calculated point of recovery post-perturbation. Trait optima are $\theta_1 = 10$ (blue population trajectory) and $\theta_2 = 5$ (red population).

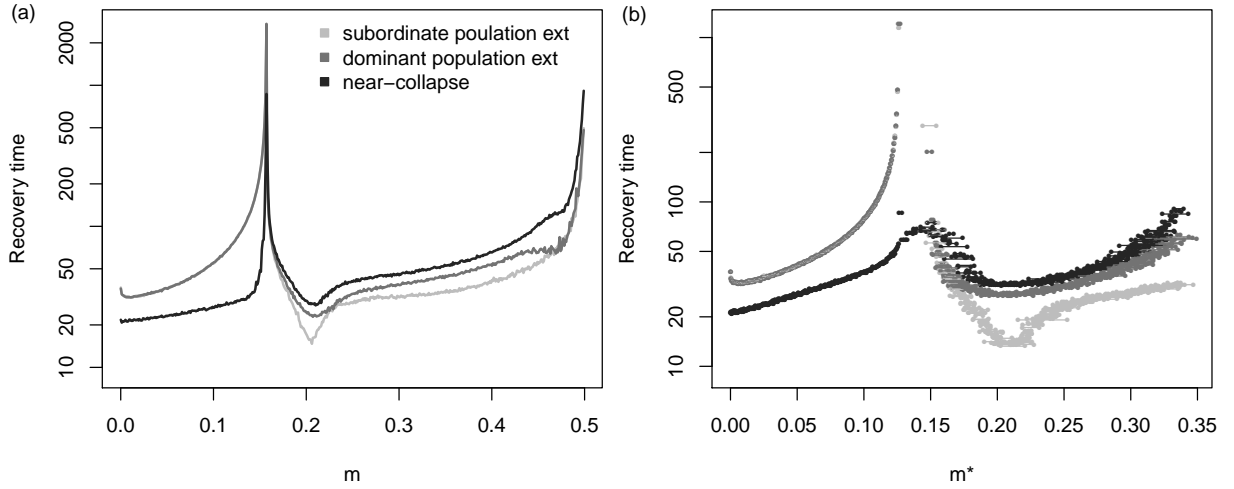


Figure S3: Recovery time of N_T following the extinction of either the low-density (light gray) or high-density (gray) population, or the near-collapse of both (dark gray) assuming (a) constant straying rates m and (b) density dependent straying rates (evaluated at the steady state m^*) with trait heritability $h^2 = 0.8$. If m is density dependent, in the alternative steady state regime there are two straying rates observed: one each for the low- and high-density populations, respectively, which are linked by a horizontal line.

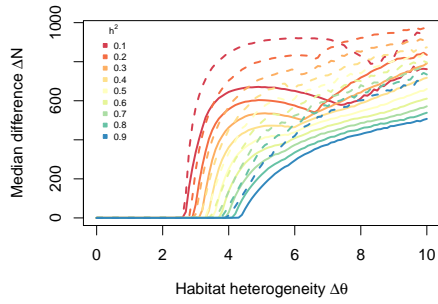


Figure S4: Median difference in population densities taken over the straying rate as a function of habitat heterogeneity $\Delta\theta$. Solid lines are for constant m ; dashed lines are for density dependent m

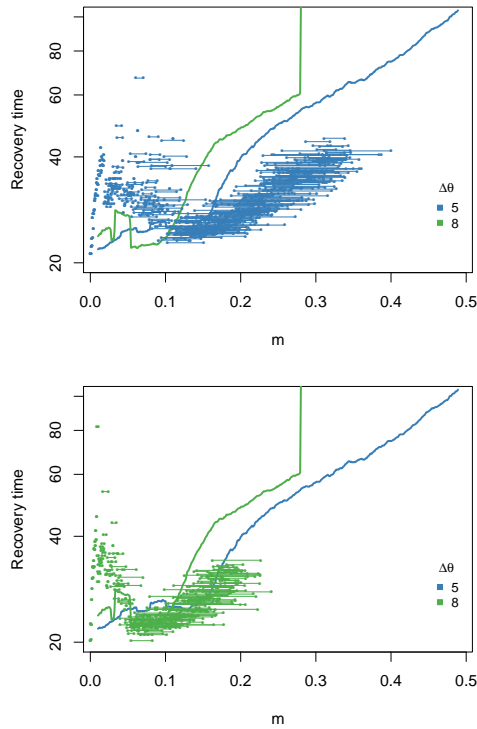


Figure S5: Recovery time as a function of straying rate m and habitat heterogeneity $\Delta\theta$.

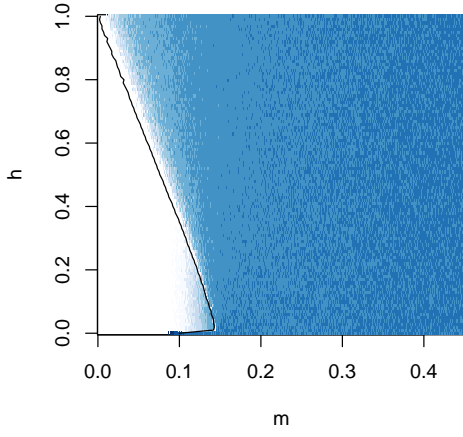


Figure S6: Distance dependent portfolio effects as a function of straying rate m and trait heritability h^2 . When straying is distance dependent, m increases as $\Delta\theta$ decreases.

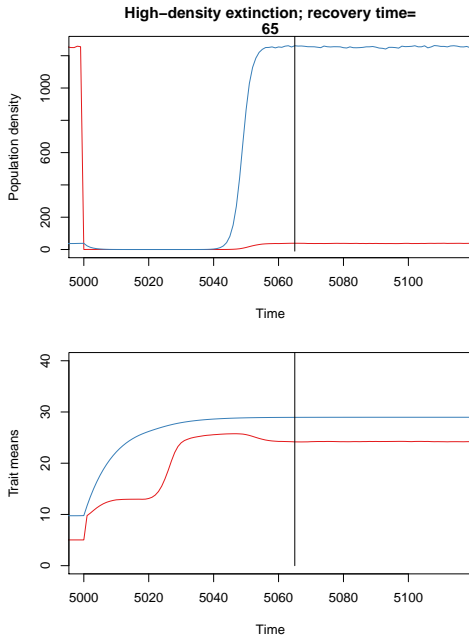


Figure S7: Distance dependent straying, where increased differences in trait optima between sites $\Delta\theta$ corresponds to lower rates of straying m . At low rates of straying $m = 0.02$ ($\Delta\theta = 24$), extinction of the dominant population leads to slower-than-expected recovery times because the subordinate population is isolated enough to evolve towards its own trait optimum until growth of the dominant population overwhelms this local selection. In this case, m is less than $m = 0.034$ (denoted by the asterisk in figure 7), such that isolation allows the subdominant population to ‘run away’ from the influence of the dominant population, leading to a switch in states.

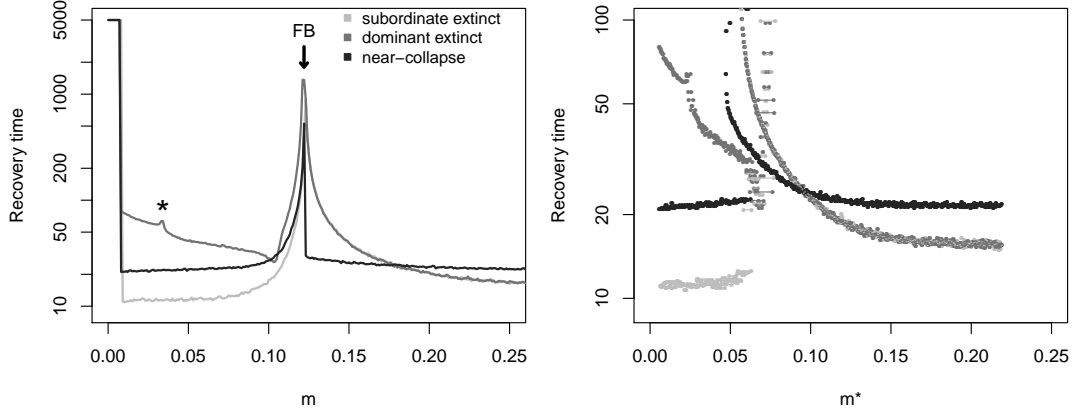


Figure S8: Distance dependent recovery times for three disturbance types. When straying is distance dependent, m increases as $\Delta\theta$ decreases for constant (a) and density dependent (b) staying rates. The fold bifurcation is not as clear in (b) because $\Delta\theta$ is a function of the individual straying rate m_0 , whereas the x-axis in (b) is the straying rate at the steady state m^* . Despite this difference, the general trends shown in (a) are also present in (b).

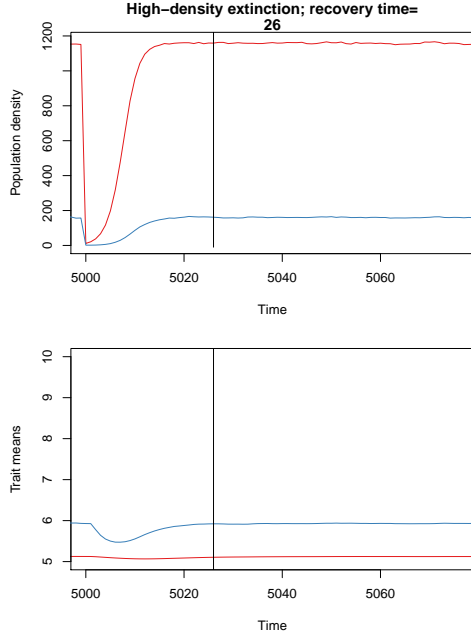


Figure S9: Near collapse of both populations with a low straying rate $m = 0.1$ and low trait heritability $h^2 = 0.2$ (see figure 5a). Black line marks the calculated point of recovery post-perturbation. Trait optima are $\theta_1 = 10$ (blue population trajectory) and $\theta_2 = 5$ (red population).